# Two-Dimensional Stress-Strain Relationship for Canine Pericardium

**Hwa Soon Choi**
Postdoctoral Fellow.

**R. P. Vito**
Associate Professor.

School of Mechanical Engineering,
Georgia Institute of Technology,
Atlanta, Ga. 30332

*Two-dimensional pseudoelastic mechanical properties of the canine pericardium were investigated* in vitro. *The pericardium was assumed to be orthotropic. The material symmetry axis was determined* a priori *and aligned with the stretching axis. Various biaxial stretching tests were then performed and a set of data covering a wide range of strains was constructed. This complete data set was fitted to a new exponential type constitutive model, and a set of true material constants was determined for each specimen. Using the constitutive model and the true material constants, the results from constant lateral force tests and constant lateral displacement tests were predicted and compared with experiment.*

## Introduction

The pericardium is a thin membrane enclosing the heart. It is known that the pericardium has a significant influence on both cardiac function and the diastolic interaction between the two chambers of heart [4, 8]. Pericardium is also used to make artificial heart valves and as a cardiac "patch." Thus, identification of the mechanical properties of the pericardium is one of the cornerstones of pericardial and cardiac mechanics.

*In vivo* measurement of pericardial pressure, geometry and boundary conditions is difficult, thus most of our knowledge regarding mechanical properties of pericardium has been obtained from *in vitro* investigations. Several uniaxial [14, 16, 18, 22] and a few biaxial [2, 9, 15] studies have been conducted on excised pericardia. These experimental studies showed that the pericardium behaved like a highly nonlinear, anisotropic and viscoelastic material. However, all previous studies were unsuccessful in reducing the experimental data to a general constitutive model, primarily because of the experimental and theoretical difficulties associated with nonlinear and anisotropic material behavior.

The pericardium appears to be at best a sheet of orthotropic membrane. In order to completely determine the constitutive law, biaxial data in which the extensional and shear strains are varied independently are needed. However, in all previous investigations of the pericardium, this generalized biaxial testing has not been performed. Instead, biaxial tests using incomplete experimental protocols have been conducted. Another fundamental problem is that the material symmetry axis of the pericardium has not been determined. Misalignment of the material symmetry axis and the stretching axis may lead to errors in the interpretation of experimental data. Moreover, published values for the material constants varied widely and were even protocol dependent primarily because of using ill-conditioned data with collinearities.

In the present study, an attempt is made to overcome these difficulties. New experimental techniques are developed, and consistent biaxial stretching tests and data analysis methods are employed to determine the two-dimensional stress-strain law for normal pericardium.

## Experimental Method

A computer-controlled biaxial testing system, an advanced version of an earlier device [11, 21], was used to investigate the mechanical properties of the pericardium. The main components of the system are the tissue bath, stretching mechanism, force measurement system and dimension measurement system. The stretching mechanism consists of two identical and orthogonally positioned axes, each driven by a digital DC servo motor. Each axis consists of two coupled, double-nut, preloaded ball screws, one with a left and one with a right hand thread; an arrangement that kept the center of the specimen fixed. The servo motor accepted velocity and position information through customized controller units and sixteen bit parallel interfaces connected to the computer (PDP 11/34). The resultant force on each axis was measured using a force transducer and an air slide which eliminated frictional forces. The output of the force transducers was conditioned and digitized with A/D converters interfaced to the computer. The dimension measurement system consisted of a video camera, a video digitizer ($640 \times 480 \times 8$ bits) and a controller unit. Using this system, the location of four particles placed on the specimen could be continuously tracked and determined.

Fresh parietal pericardia were obtained from healthy dogs of varying sex, age, and weight. Prior to removal, pericardia were marked using sutures to indicate their anatomical orientation. Tissues were stored in saline at 5°C and used within 24 hours of removal. A circular specimen was prepared to determine the material symmetry axis prior to biaxial stretching tests. Using the whole pericardium, the largest possible uniform and flat portion was excised. The excised tissue was laid un-

Contributed by the Bioengineering Division for publication in the JOURNAL OF BIOMECHANICAL ENGINEERING. Manuscript received by the Bioengineering Division May 15, 1989; revised manuscript received January 2, 1990.

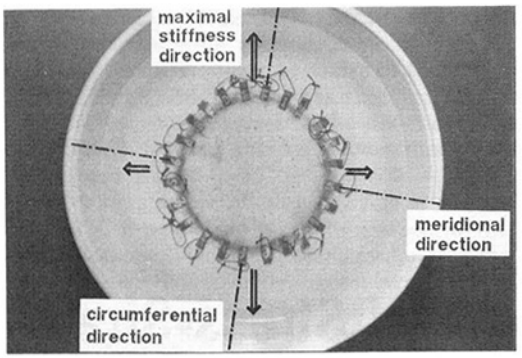


**Fig. 1 Shown is a photograph of a marked circular specimen in its undeformed state. The material symmetry axes (arrows) are identical to the major and minor axes of the ellipse. The anatomical directions (meridional and circumferential) are also shown.**

deformed on a lexan plate and a 7.0 cm diameter circle marked on the tissue. Careful dissection resulted in a circular specimen to which 000-silk sutures were attached, using magnetic cassette tape and super glue, at 15 deg increments as shown in Fig. 1. The anatomical orientation of the tissue was marked on the tape.

The specimen was mounted in the testing device and a small tension of 0.00098 N (0.1 gg) was applied along a diameter after which its length was held constant. A tension of 0.98 N (100 gg) was then applied along the diameter orthogonal to it. This actually resulted in imposing a 0.20 to 0.34 N along the former diameter. Using a mixture of enamel ink and super glue, two marks 5.0 cm apart were made on the tissue centered along the diameter subjected to 0.98 N. The circular specimen was then rotated 15° and the procedure repeated until all possible diameters were loaded and marked. When the tissue was allowed to return to the stress-free state, the marks placed on the tissue formed an ellipse having major and minor axes coincident with the unknown material symmetry axes, as shown in Fig. 1. The angle between the material symmetry axes and the pre-marked meridional direction of the heart was measured with a protractor to an accuracy of 7.5 deg.

For the biaxial stretching tests, an approximately 4.0 cm × 4.0 cm square specimen was cut along the material symmetry axes from the circular specimen. On the 1.0 cm × 1.0 cm square central region of the specimen, approximately 200$\mu$m diameter black particles were glued, one at the center and one at each of four corners. Silk sutures were attached to the specimen as described above. The specimen was then immersed in a saline bath and mounted in the biaxial stretching device. After mounting the specimen in the experimental device, care was taken to obtain the stress-free state as an initial reference state. In order to assure that all sutures were taut, a stretching force of 0.0098 N (0.1 gg) was imposed in each stretching direction. This state was defined as a reference state from which all subsequent biaxial stretching tests were started. The position of tracking particles in the reference state was determined by locating particles using a joystick cursor. A typical particle occupied approximately 7 × 7 pixels, and the centroid of each particle was determined using the row and column method [11] with an accuracy of ±0.03 mm. During the subsequent biaxial tests, stretching forces and the location of tracking particles are continuously measured and recorded.

To identify the two-dimensional stress-strain law of the pericardium, four classes of biaxial testing were conducted on each specimen at room temperature. First, a series of equibiaxial stretching tests were performed. Five initial preconditioning cycles were imposed on the specimen at the stretching rate of 0.00381 cm/s and a maximum stretching force of 0.98 N. One additional loading-unloading cycle was performed and the data stored. Three more equibiaxial stretching tests were conducted after changing the stretching rate to 0.000635, 0.00381, and 0.0127 cm/s, respectively, in each test. The second series of tests consisted of non-equibiaxial stretching tests. Both axes were stretched at various combinations of stretching rates such as $v_1/v_2 = 25/30$, 30/25, 20/30, 30/20, 15/30, 30/15, 10/30, 30/10, 5/30 and 30/5, where $v_i (i = 1, 2)$ represents the stretching rate of axis $i$ and a value of 30 is equivalent to 0.00381 cm/s. Combinations of stretching rates ($v_1$, $v_2$) for the equibiaxial and non-equibiaxial protocols and the resulting strain ratios ($E_{22}/E_{11}$) are given for all specimens in Table 1. In fact, the same combination of stretching rates ($v_1$, $v_2$) resulted in different strain ratios ($E_{22}/E_{11}$) for different specimens because the specimens and their central tracking regions were not exactly square and their dimensions had some interspecimen variations. In each test, two loading-unloading cycles were repeated and data from the second cycle were recorded. Two additional tests were conducted. In the first, one direction was stretched at a constant rate while the displacement of the second direction was held constant. In the other, one direction was stretched at a constant rate while the force in the orthogonal direction was maintained at a prescribed level. Since the material symmetry axis and the stretching axis were coincident, these experiments were referred to as the "0 deg-experiment."

After completion of these experiments, the specimen was removed from the experimental device. A second square specimen was then prepared. An approximately 2.8 cm × 2.8 cm square loading region was generated by cutting the original specimen along lines 2.1 cm in length joining two points on adjacent sides. The sides of this "new" specimen make angles of 45 deg with the material symmetry axis, hence equibiaxial experiments performed with this sample were referred to as the "45 deg-experiment."

At the end of biaxial stretching tests, the thickness of the specimen was measured using an electrical resistance micrometer. A new technique was developed to minimize the difficulties resulting from squeezing and drying of the tissue and fluid surface tension effects. The micrometer was advanced until a voltmeter indicated that contact with the saline film on the tissue was made. A reading was taken and the micrometer was withdrawn from the tissue. A second reading was taken when the voltmeter indicated that contact with the saline film was broken. The difference between these two readings was a measure of the surface tension effect. As the saline film evaporated, this effect diminished. However, some saline must always be present on the tissue to prevent drying and the associated change in mechanical properties. Therefore, measurements taken over ten minutes were extrapolated using linear regression. The intersection of two straight lines determines the thickness of the tissue. A detailed description of measurement technique and results may be found in [3].

## Data Analysis

There were approximately 200 data points for each loading-unloading cycle. Only the loading part of the data was analyzed. The original data of stretching forces and particle positions were converted to stress-strain data. Lagrangian stresses ($T_{11}$, $T_{22}$, $T_{12}$, $T_{21}$) were calculated from the measured stretching forces ($F_1$, $F_2$) and the initial cross sectional area:

$$T_{11} = \frac{F_1}{L_{20} h_0}, \quad T_{22} = \frac{F_2}{L_{10} h_0}, \quad T_{12} = T_{21} = 0$$

where, $h_0$ was the initial thickness and $L_{10}$ and $L_{20}$ were initial lengths of the specimen. The Kirchhoff stresses ($S_{11}$, $S_{22}$, $S_{12}$) directly followed from the above [7]:

$$S_{11} = \frac{C_{22}}{C_{11}C_{22} - C_{12}C_{21}} T_{11}$$

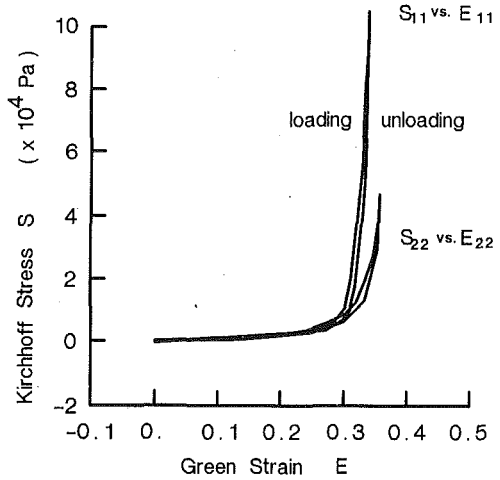


**Fig. 2 Two stress-strain curves in this figure are representative equibiaxial stretching results. Hysteresis and anisotropic behavior are evident.**

$$S_{22} = \frac{C_{11}}{C_{11}C_{22} - C_{12}C_{21}} T_{22}$$

$$S_{12} = \frac{-C_{21}}{C_{11}C_{22} - C_{12}C_{21}} T_{11}$$

where $C_{ij}(i, j = 1, 2)$ were deformation gradients [7] which could be calculated from the displacements of the four tracking particles using interpolation functions [10, 11]. Green strains ($E_{11}$, $E_{22}$, $E_{12}$) were given by [7]:

$$E_{ij} = \frac{1}{2}(C_{ri}C_{rj} - \delta_{ij})$$

where $\delta_{ij}$(i, $j = 1, 2$) is the Kronecker delta. The $C_{12}$ and $C_{21}$ at the center of specimen were close to zero in all 0 deg-experiments. A pure homogeneous deformation was assumed in the "0 deg-experiment" and shear strains were neglected in the analysis.

A stress-strain data set from one loading protocol was reduced in size by sampling 15 data points; eight at low strains and seven at high strains. This reduced data set was transferred to the main computer (CDC Cyber) for analysis. An individual data set obtained using a specific loading protocol has a collinearity [1]; a near linear relationship between independent variables. The presence of collinearity in a data set leads to unstable and almost meaningless regression coefficients [1]. Therefore, an individual data set cannot be used alone for the regression analysis. To remedy this problem, a complete data set which covered the whole range of the independent variables was constructed for each specimen by accumulating all the reduced data from the various stretching tests.

The following form of strain energy density function $W$ was found to give a good fit to the observed data [3]:

$$W = B_0\left\{e^{\frac{1}{2}b_1E_{11}^2} + e^{\frac{1}{2}b_2E_{22}^2} + e^{b_3E_{11}E_{22}} - 3\right\}$$

where $B_0$, $b_1$, $b_2$, and $b_3$ were the material constants. The assumed theoretical Kirchhoff stresses $S_{11}$ and $S_{22}$ followed directly from W [7]:

$$S_{11} = \frac{\partial W}{\partial E_{11}} \qquad S_{22} = \frac{\partial W}{\partial E_{22}}$$

This constitutive model was particularly suitable for fitting highly nonlinear data over a wide range of strains, while preserving the cross product term and satisfying the material symmetry arguments. The parameter $B_0$ had some correlation with the other parameters $b_1$, $b_2$, and $b_3$. However, it was not sufficient to cause any numerical instability, and the dropping of $B_0$ made it difficult to get a good fit to the data.

**Table 1 Comparison of the material constants determined using individual data sets with collinearity and determined using a complete data set without collinearity is made for each specimen.**

| DOG # | SET # | PROTOCOL Stretch rates ($v_2$:$v_1$) | PROTOCOL $E_{22}/E_{11}$ | $B_0$ (Pa) | $b_1$ | $b_2$ | $b_3$ | RRMS (x $10^4$ Pa) |
|---|---|---|---|---|---|---|---|---|
| | P 1 | 30:10 | 2.77 | 19.1 | 163.13 | 42.64 | 35.97 | 0.39 |
| | P 2 | 30:15 | 1.94 | 74.2 | 63.39 | 32.78 | 22.38 | 0.37 |
| # | P 3 | 30:30 | 0.92 | 479.1 | 10.53 | 10.78 | 15.87 | 0.16 |
| 0 | P 4 | 15:30 | 0.33 | 585.5 | 34.48 | 78.77 | 31.03 | 0.25 |
| 1 | P 5 | 10:30 | 0.13 | 17.2 | 42.31 | 277.58 | 64.32 | 0.28 |
| | Set (P1+..+P5) | | | 186.7 | 26.28 | 25.75 | 17.91 | 0.37 |
| | P 1 | 30:15 | 3.26 | 0.6 | -561.91 | 296.35 | 511.61 | 0.66 |
| | P 2 | 30:20 | 2.52 | 2.6 | -412.17 | 272.55 | 391.89 | 0.49 |
| | P 3 | 30:25 | 1.62 | 2.9 | 855.25 | 63.41 | 361.77 | 0.25 |
| # | P 4 | 30:30 | 1.32 | 2.1 | 1003.34 | 168.88 | 367.13 | 0.20 |
| 0 | P 5 | 25:30 | 0.97 | 0.7 | 1088.52 | 241.17 | 430.34 | 0.28 |
| 4 | P 6 | 20:30 | 0.73 | 4.4 | 790.86 | 186.64 | 343.37 | 0.43 |
| | P 7 | 15:30 | 0.58 | 1.1 | 905.16 | -79.72 | 442.02 | 0.56 |
| | Set (P1+..+P7) | | | 12.9 | 628.95 | 199.46 | 294.82 | 1.16 |
| | P 1 | 30: 5 | 5.82 | 8.0 | 1344.69 | 120.38 | 242.21 | 0.26 |
| | P 2 | 30:10 | 3.89 | 14.4 | 213.95 | 117.67 | 184.68 | 0.20 |
| | P 3 | 30:15 | 2.72 | 44.7 | - 8.53 | 113.09 | 150.86 | 0.26 |
| | P 4 | 30:20 | 1.84 | 54.8 | -313.50 | 118.09 | 146.58 | 0.42 |
| | P 5 | 30:25 | 1.63 | 21.3 | 324.32 | 24.06 | 178.74 | 0.23 |
| # | P 6 | 30:30 | 1.22 | 5.3 | 556.71 | 31.54 | 227.86 | 0.31 |
| 0 | P 7 | 25:30 | 1.15 | 8.4 | 536.03 | 32.51 | 205.43 | 0.35 |
| 6 | P 8 | 20:30 | 0.98 | 6.3 | 587.85 | 30.61 | 201.19 | 0.29 |
| | P 9 | 15:30 | 0.88 | 9.5 | 554.86 | - 43.85 | 186.75 | 0.56 |
| | P10 | 10:30 | 0.73 | 10.1 | 552.20 | 54.36 | 174.55 | 0.25 |
| | P11 | 5:30 | 0.46 | 7.9 | 565.73 | 284.80 | 194.68 | 0.35 |
| | Set (P1+...+P11) | | | 44.4 | 385.37 | 85.46 | 148.15 | 1.11 |
| | P 1 | 30:15 | 2.01 | 20.5 | 45.37 | 26.55 | 26.85 | 0.22 |
| | P 2 | 30:20 | 1.54 | 43.2 | 25.32 | 24.32 | 22.96 | 0.12 |
| | P 3 | 40:30 | 1.28 | 47.7 | 22.47 | 21.49 | 22.05 | 0.09 |
| # | P 4 | 35:30 | 1.08 | 36.4 | 33.31 | 24.06 | 23.47 | 0.14 |
| 0 | P 5 | 30:30 | 0.91 | 16.1 | 39.38 | 33.23 | 26.86 | 0.20 |
| 8 | P 6 | 30:35 | 0.73 | 9.3 | 41.62 | 47.14 | 29.60 | 0.22 |
| | P 7 | 25:35 | 0.62 | 1.2 | 51.45 | 83.22 | 39.08 | 0.28 |
| | P 8 | 10:30 | 0.28 | 3.0 | 43.17 | 262.30 | 39.15 | 0.16 |
| | Set (P1+...+P8) | | | 55.8 | 26.05 | 21.15 | 20.60 | 0.38 |
| | P 1 | 30: 5 | 21.15 | 0.002 | 1575.60 | 93.81 | 272.53 | 0.37 |
| | P 2 | 30:10 | 5.86 | 0.430 | 498.13 | 62.58 | 105.95 | 0.26 |
| | P 3 | 30:15 | 2.74 | 0.156 | 174.35 | 70.61 | 83.73 | 0.30 |
| | P 4 | 30:20 | 1.71 | 2.045 | - 0.02 | 55.93 | 52.55 | 0.46 |
| | P 5 | 30:25 | 1.26 | 0.168 | 132.21 | 48.61 | 69.35 | 0.25 |
| # | P 6 | 30:30 | 0.99 | 0.098 | 161.79 | 110.83 | 80.83 | 0.30 |
| 0 | P 7 | 25:30 | 0.82 | 0.116 | 146.95 | 22.91 | 82.38 | 0.56 |
| 9 | P 8 | 20:30 | 0.67 | 0.124 | 144.63 | 99.33 | 85.24 | 0.17 |
| | P 9 | 15:30 | 0.43 | 0.005 | 178.13 | 157.95 | 137.70 | 0.31 |
| | P10 | 10:30 | 0.31 | 0.235 | 126.99 | 200.01 | 100.83 | 0.20 |
| | P11 | 5:30 | 0.17 | 1.276 | 97.49 | 99.39 | 91.04 | 0.28 |
| | Set (P1+...+P11) | | | 63.60 | 53.88 | 30.14 | 32.38 | 1.16 |

For each specimen, a complete data set was fitted to the assumed constitutive model using a nonlinear least square method, and a set of true material constants was determined. The test results under different loading protocols were then predicted and compared with the experimental data.

## Results

A representative mechanical response of normal pericardium subjected to equibiaxial stretching is shown in Fig. 2. This figure demonstrates several characteristic features. First, the stress-strain curves are highly nonlinear, showing a considerable tissue compliance at small strains but a rapid stiffening at large strains. Second, there exists some hysteresis as indicated by the difference between the loading and unloading curves. Third, the stress-strain curve in one direction is different from that in the orthogonal direction. This anisotropic behavior is especially apparent at high strains. When the same specimen was stretched equibiaxially at different rates from 0.000635 cm/s to 0.0127 cm/s, strain rate had no significant effect on the stress-strain curve [3].

The variability of the material constants reported in most previous studies [2, 12, 23] was primarily due to ill-conditioned data with collinearities. In order to demonstrate this point, fitting results using individual data sets with collinearity were compared quantitatively and graphically with those obtained using a complete data set without collinearity. The material constants determined using individual data sets and a complete

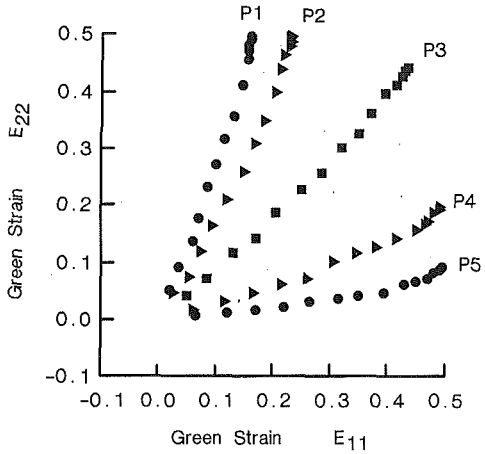


**Fig. 3 Five loading protocols (strain trajectories) used in biaxial stretching tests on specimen #01 are shown. In each test, the ratio of strains $E_{22}/E_{11}$ is almost constant.**

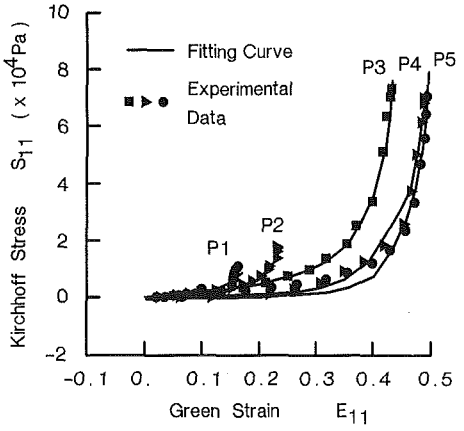


**Fig. 4(*a*)**

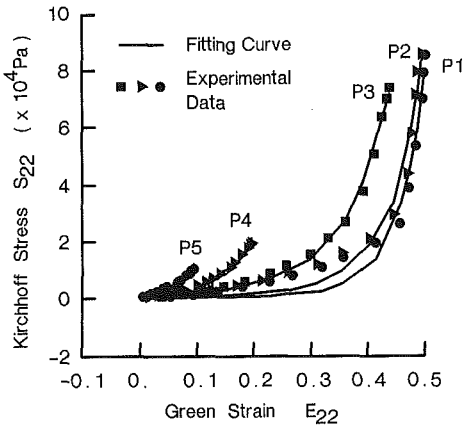


**Fig. 4(*b*)**

**Fig. 4 Curves in the figure represent the individual curve-fitting results for five different loading protocols shown in Fig. 3 for specimen #01. Five sets of curve fitting constants for the proposed model were used to fit five curves respectively: (a) $S_{11}$ versus $E_{11}$ curves and (*b*) $S_{22}$ versus $E_{22}$ curves.**

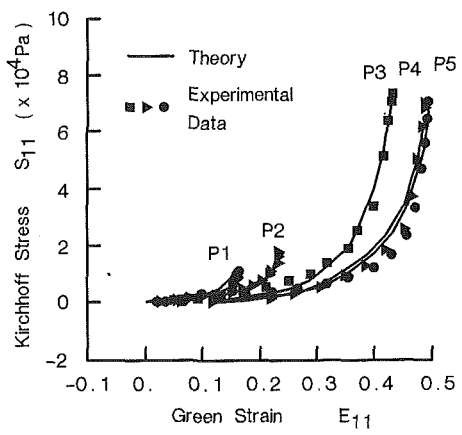


**Fig. 5(*a*)**

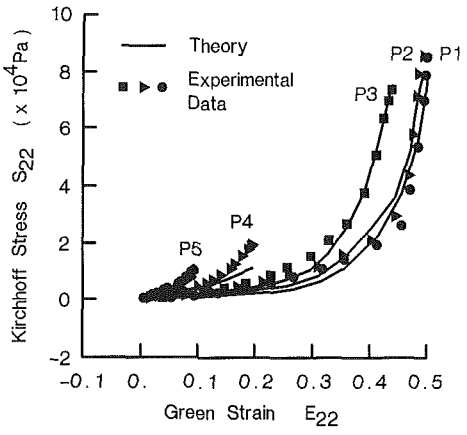


**Fig. 5(*b*)**

**Fig. 5 Curves in the figure represent the simultaneous surface-fitting results for five different loading protocols shown in Fig. 3 for specimen #01. A set of true material constants for the proposed model was used to fit five curves simultaneously: (*a*) $S_{11}$ versus $E_{11}$ curves and (*b*) $S_{22}$ versus $E_{22}$ curves.**

data set for each specimen are given in Table 1. Note that the collinearity, represented as a constant value of $E_{22}/E_{11}$, exists between the strain data in each individual data set.

When fitting an individual data set, several points were recognized. First, when different sets of initial estimator values wee used, sometimes different sets of fitting constants were obtained. Thus, the fitting constants determined using the same set of initial estimator values are given in Table 1. However, these constants are not unique even for the same loading protocol. Second, it was sometimes difficult to obtain any convergent solution because of the singularity [1] associated with collinearity. Third, the constant $b_1$ was very unstable when fitting an individual data set with high values of $E_{22}/E_{11}$, whereas $b_2$ was unstable when fitting data with low values of $E_{22}/E_{11}$. High values of $E_{22}/E_{11}$ meant that all $E_{22}$ and $S_{22}$ values in a data set are much larger than $E_{11}$ and $S_{11}$ values. Hence, even large changes in $b_1$ did not improve the fitting results and the estimated constant $b_1$ was unstable.

As a representative result, fitting results for specimen #01 are illustrated in Figs. from 3 to 5. Figure 3 shows five different loading protocols P1, P2, P3, P4, and P5, from which the corresponding five individual data sets were obtained. Figure 4(*a*, *b*) shows the individual curve fitting results in which five different sets of fitting constants were used to fit five curves respectively. On the other hand, the surface fitting results, in which a set of true material constants for the proposed model was used to fit five curves simultaneously, are shown in Fig. (5*a*, *b*). The average RRMS (residual root mean squares) value for individual curve-fitting was $0.29 \pm 0.08 \times 10^4$ **Pa**, whereas it was $0.37 \times 10^4$ **Pa** for a simultaneous surface-fitting. Comparing the RRMS values (order of $0.3 \times 10^4$ **Pa**) with the maximum stress value (order of $9.0 \times 10^4$ **Pa**), the fitting results were quite good in both cases.

However, the constants determined using an individual data set for a specific loading protocol did not fit the data obtained from other loading protocols. Figure 6 shows typical results indicating that the fitting constants determined for an equibiaxial stretching protocol (P3) did not fit the data from other

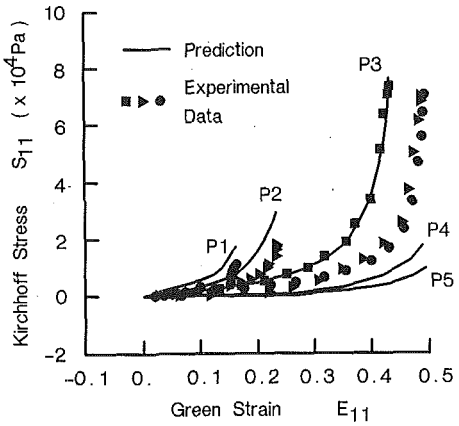


**Fig. 6 The curve fitting constants, determined using an individual data set with a specific loading protocol P3, cannot fit the data other than that for protocol P3 for specimen #01**

loading protocols (P1, P2, P4, P5) for the same specimen #01. On the other hand, a set of true material constants for specimen #01 yielded consistently good fits, as shown in Fig. 5(*a*, *b*). These fitting results indicated that the constants determined using an individual data set were not the "material constants" but the somewhat arbitrary "fitting constants."

We seek a model and a set of pseudoelastic material constants capable of describing any type of biaxial deformation. In the present study, a set of true material constants was determined using a complete data set for each specimen. If these constants are the "true" material constants, any type of biaxial deformation can be predicted using these pseudoelastic material constants. In order to check this point, the ability of material constants to fit the data obtained from a separate test was examined. Two different types of tests, constant lateral force tests and constant lateral displacement tests, were conducted on specimens #06, #09. Experimental data obtained during these tests were compared with the theoretical stress values predicted using the true material constants in the constitutive model. As typically shown in Fig. 7(*a*, *b*), a set of true material constants in the proposed model resulted in a reasonable fit to the data from different tests on the same specimen #09.

The pericardium was assumed as an orthotropic membrane, and its material symmetry axis was determined experimentally prior to biaxial stretching tests. Thus, the material symmetry axis was coincident with the stretching axis of the device during the "0 deg-experiment". When equi-biaxial forces were imposed on specimen #09 during the "0 deg-experiment", the strains in both axes were significantly different. On the other hand, the test results on the same specimen during the "45 deg-experiment" indicated that the stiffnesses in both the ±45 deg directions from the material symmetry axis were almost identical, as shown in Fig. 8. This fact demonstrated that the specimen was orthotropic.

Most canine pericardia showed some degree of anisotropy whereas some were close to isotropic. The degree and direction of anisotropy showed significant specimen-to-specimen variation as summarized in Table 2. In order to compare the degree of orthotropy among specimens, two indices R1 and R2 were introduced.

As a byproduct of the determination of the material symmetry axis, the maximum strains in the stiff direction and the compliant direction were measured. The different maximum strains in both axes under the same loading condition indicate the presence of anisotropy. Thus, the orthotropy index R1 was defined as the ratio of the maximum strains in both axes. That is,

$$R1 = \frac{E_{22\max}}{E_{11\max}}$$

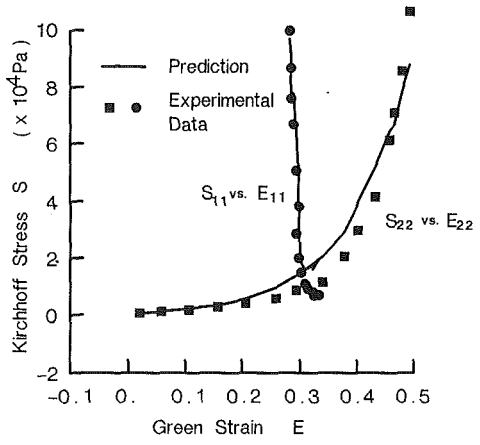


**Fig. 7(*a*)**

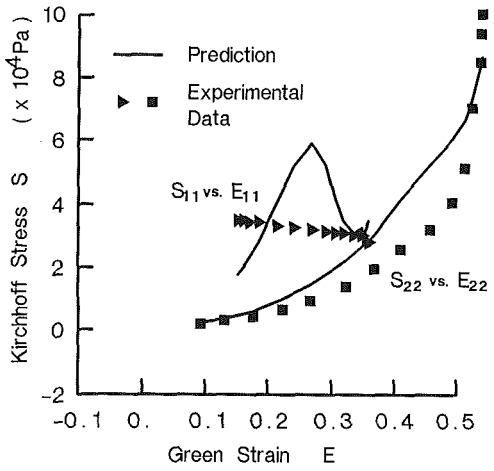


**Fig. 7(*b*)**

**Fig. 7 Prediction of different test results are made using the proposed constitutive model and a set of true material constants for specimen #09: (*a*) constant lateral displacement test and (*b*) constant lateral force test.**

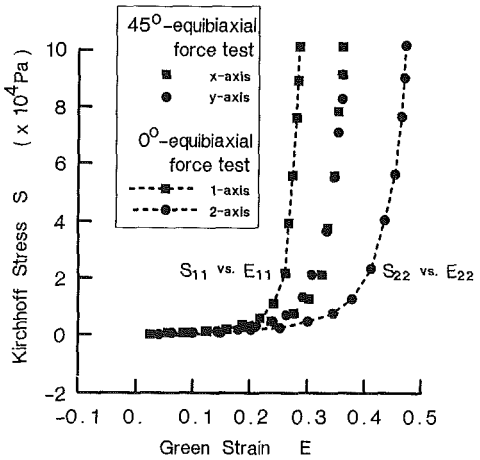


**Fig. 8 The comparison of the results of the "0 deg-experiment" and "45 deg-experiment" is shown. When the material symmetry axes are coincident with the stretching axes (0 deg-experiment), the anisotropic behavior is apparent. However, when the same specimen is stretched along the direction 45 deg from the material symmetry axes (45 deg-experiment), the stiffnesses in both stretching directions are almost identical.**

where $E_{11\max}$ is obtained at force $F_1 = 0.98$ N in the absence of $E_{22}$ ($E_{22} \simeq 0$) and $E_{22\max}$ is obtained at force $F_2 = 0.98$ N in the absence of $E_{11}$ ($E_{11} \simeq 0$).

The proposed constitutive model has a characteristic that

**Table 2 Quantification of material symmetry axes and the degree of orthotropy are given in this table. The 5.0 cm-long marks stamped at the prescribed loading condition were reduced to the measured lengths of the major and minor axes at a stress-free state. The orthotropy index R1 was determined from these measured lengths, whereas another index R2 was estimated from the true material constants for the proposed model.**

| Specimen | Anatomical orientation of the max. stiffness dir. | Length (cm) major axis | Length (cm) minor axis | Orthotropy Index R1 $E_{22m}/E_{11m}$ | Orthotropy Index R2 $\sqrt{b_1/b_2}$ |
|---|---|---|---|---|---|
| | (meridional dir. of the heart) | | | | |
| #01 | unknown | not measured | | not measured | 1.0 |
| #04 | 45° | 4.1 | 3.8 | .36/.24 = 1.5 | 1.7 |
| #06 | 0° | 4.3 | 3.8 | .36/.17 = 2.1 | 2.1 |
| #08 | unknown | 3.4 | 3.3 | .64/.58 = 1.1 | 1.1 |
| #09 | 82.5° | 3.5 | 3.3 | .64/.52 = 1.2 | 1.3 |

the anisotropic behavior can be accounted by the different contribution of material constants $b_1$ and $b_2$ to the strain energy. Thus, based on our constitutive model, we propose a theoretical orthotropy index R2 which could be easily estimated from the true material constants [3]:

$$R2 = \sqrt{\frac{b_1}{b_2}}$$

As shown in Table 2, there exists a good agreement between the experimentally measured index R1 and the theoretically estimated index R2. When both indices are close to 1.0, the specimen can be regarded as an isotropic material. For example, specimen #08 is almost isotropic with an index of 1.1, whereas specimen #06 is anisotropic with an index of 2.1.

## Discussion

Identification of stress-strain relationships of biological tissues has been hampered by experimental and theoretical difficulties. Pericardium is so highly nonlinear and anisotropic that the experimental measurements of thickness, reference dimensions, strain and stress require careful consideration.

The pericardial thickness reported in the previous studies [2, 5, 14, 15] ranges from 0.14 to 0.30 mm probably owing to differences in the measurement techniques used. In the present study, the average pericardial thickness for seven specimens was $0.262 \pm 0.022$ mm. This value is slightly smaller than that estimated by Freeman and LeWinter [5], but larger than that reported by Wiegner et al. [22] and Lee et al. [15]. In [15], the thickness was measured under a pressure of approximately 3 mmHg, which may have led to the smaller values reported. For this reason, thickness was measured in the stress-free state while avoiding drying and surface tension effects.

The determination of the initial reference dimensions is difficult and represents one of the most probable sources of errors in biaxial experiments. Since the pericardium is very compliant at a low stress level, even a very small load can produce substantial strains. Therefore, every attempt was made to attain the stress-free state by observing the changes in output of the force transducers. Although the force measurement was accurate to 0.00049 N (0.05 gm), this task was complicated by noise and drift in the force transducers and signal conditioners, very small differences in the length of the sutures, and the tissue's own weight. Given this reality, an additional force of 0.00098 N (0.1 gm) was imposed biaxially on the specimen and this state was defined as the initial reference state for all tests. Notice that the initial particle positions were determined in the reference state before preconditioning. The reference dimension was defined after preconditioning in most of previous studies [6, 12, 13, 15]. However, some evidence exists that the deformation caused by preconditioning is not permanent and may even vary between protocols [13, 18]. Since a unique reference dimension is assumed to exist for a pseudoelastic material in this study, the reference dimensions were defined before preconditioning.

Basic considerations of the experimental design and data processing have sometimes been overlooked in biomechanics. In order to quantify the two-dimensional constitutive relationship of an anisotropic membrane, it is essential to obtain the data in which two independent variables, $E_{11}$ and $E_{22}$ are randomly distributed. Although our data set does not satisfy the condition of randomness, it does avoid collinearities common in previous studies [2, 12, 17, 20, 23, 24]. In most studies [2, 12, 24], the numerical instability due to the collinearity could not be avoided and resulted in wide variations of the estimated material constants for the same specimen. For example, the data in [2, 24] had the linear relationship of $E_y = kE_x$. In this case, parameters $A_x$ and $A_y$ can not be uniquely determined, but rather the linear combination $A_x + k^2 A_y$. Vaishnav et al. [19] and Fung et al. [6] pointed out the importance of obtaining data covering a wide range of strains to avoid ill-conditioning. In [6], a set of data which included only two loading protocols was used and hence was not sufficient to avoid the problems related to collinearity. Thus, when using different data sets, different sets of material constants were estimated. Fung et al. [6] were also unsuccessful in using a set of constants determined by one sequence of experiments, in trying to predict the outcome of other experiments on the same specimen, and concluded that the tissue was inelastic. This conclusion can be justified only when accurate and sufficient experimental data are fitted to the correct form of constitutive model. However, no consensus exists on the correct form of constitutive model and the optimal way of experimental testing.

To describe the mechanical properties of biological tissues as accurately and concisely as possible, many different types of constitutive models have been suggested [3, 6, 9, 10, 19, 23, 24]. However, a complete constitutive model which is capable of describing any type of deformation is not available. Fung's equation [6, 11, 17, 20, 24] has been widely used to fit highly nonlinear data over a wide range of strains because it has a simple form and still satisfies the requirements of being positive definite and symmetric [11]. In the present investigation, an attempt was made to fit sets of data using Fung's equation. However, Fung's equation resulted in negative or very small coefficients for the cross product terms [3]. This may be primarily a numerical artifact due to a constraint imposed by the inseparable quadratic powers of strains. This same phenomenon was also observed by Yin et al. [23, 24] and Humphrey et al. [11, 12], thus the cross product terms in exponentials were dropped in their strain energy density functions. Using the exponential function without cross product terms [24] misleadingly predicts that the stress in the unstretched direction should remain zero even when the other direction is stretched. The mixed polynomial-exponential functions [2, 23, 11, 12] contain cross product terms only in the polynomial portion. Thus, the stress in the unstretched direction is not zero but a linear function of the orthogonal strain. However, this feature still imposes a theoretical limitation at high strains. Therefore, this type of strain energy function cannot cover a wide range of strains simultaneously and cannot

account for in-plane coupling effects at high strains. On the other hand, the strain energy density function introduced in the present study involves separable exponentials of quadratic strains. By using this function, all the estimated material constants were positive. Since the constitutive model still involves cross product terms, in-plane coupling effects may be accounted for and quantified.

The pericardium was considered to be orthotropic in most recent studies [2, 15, 22, 23]. It was found that every specimen showed some degree of anisotropy. Although some authors [9, 14] assumed the pericardium was isotropic, their experimental results indicated the presence of some degree of anisotropy. Wiegner et al. [22] concluded that the greatest stiffness consistently lay in the direction 45 deg counterclockwise from the circumferential direction of heart. Contrary to this conclusion, the present investigation did not indicate any consistent anatomical orientation of maximum stiffness. In the present study, the direction of maximum stiffness varied from specimen to specimen as observed by Lee et al. [15]. Although the pericardium was considered to be orthotropic in some previous studies, the material symmetry axis was not determined, but simply assumed to be coincident with their experimental stretching axis [2, 23]. If an orthotropic specimen was stretched along the 45 deg-direction from the material symmetry axis, the experimental results might be misleadingly interpreted as exhibiting isotropy. For this reason, it is important that the material symmetry axis should be determined *a priori* and the stress-strain data should be referred to a specified direction. Lee et al. [15] claimed that they determined the material symmetry axis by observing the deformation of a marked 6-8 mm diameter circle into an ellipse while imposing 200 gram equibiaxial forces. The present investigators found that this technique gave variable results probably because of the difficulties associated both with placing markers on the tissue while in the stress-free state and imposing equibiaxial stresses continuously without acknowledging the material symmetry axis. The technique used in the present study was effective in minimizing these difficulties.

Although some problems remain to be solved, the present methodology yields the true material constants which are capable of describing mechanical responses over a wide range of strains and assessing the degree of orthotropy.

## Acknowledgments

Appreciation is expressed to Ms. Lynn Dorsey and her staff at the Cardiothoracic Research Laboratory (Crawford Long Hospital, Atlanta, GA) for their help with the pericardial specimens used in these experiments. This work was supported in part by a grant from the American Heart Association, Georgia Affiliate.

## References

1 Belsely, D., Kuh, E., and Welsch, R., *Regression Analysis: Identifying Influential Data and Sources of Collinearity*, Wiley, New York, 1980.

2 Chew, P. H., Yin, F. C. P., and Zeger, S. L., "Biaxial Stress-strain Properties of Canine Pericardium," *J. Mol. Cell Cardiol.*, Vol. 18, 1986, pp. 567-578.

3 Choi, H. S., "Mechanical Properties of Canine Pericardium," Ph.D. thesis, 1989, Georgia Institute of Technology.

4 Fowler, N. O., *The Pericardium in Health and Disease*, Futura Publishing Company, Inc., N.Y., 1985.

5 Freeman, G. L., and LeWinter, M. M., "Pericardial Adaptions during Chronic Cardiac Dilation in Dogs," *Circ. Res.*, Vol. 54, 1984, pp. 294-300.

6 Fung, Y. C:, Fronek, K., and Patitucci, P., "Pseudoelasticity of Arteries and the Choice of its Mathematical Expression," *Am. J. Physiol.*, Vol. 237, No. 5, 1979, pp. H620-631.

7 Green, A. E., and Adkins, J. E., *Large Elastic Deformations*, (2nd ed.) Clarendon Press, Oxford, 1970.

8 Hess, O. M., Bhargava, V., Ross, J. Jr., and Shabetai, R., "The Role of the Pericardium in Interactions between Cardiac Chambers," *Am. Heart J.*, Vol. 106, 1983, pp. 1377-1383.

9 Hildebrandt, J., Fukaya, H., and Martin, C. J., "Stress-strain Relations of Tissue Sheets Undergoing Uniform Two-Dimensional Stretch," *J. of Appl. Physiol.*, Vol. 27, No. 5, 1969, pp. 758-762.

10 Hoffman, A. H., and Grigg, P., "A Method for Measuring Strains on Soft Tissue," *J. Biomechanics*, Vol. 17, No. 10, 1984, pp. 795-800.

11 Humphrey, J. D., "Mechanical Behavior of Excised Visceral Pleura," Ph.D. thesis, Georgia Institute of Technology, 1985.

12 Humphrey, J. D., Vawter, D. L., Vito, R. P., "Pseudoelasticity of Excised Visceral Pleura," ASME JOURNAL OF BIOMECHANICAL ENGINEERING., Vol. 109, 1987, pp. 115-120.

13 Lanir, Y., and Fung, Y. C., "Two Dimensional Mechanical Properties of Rabbit Skin II.-Experimental Results," *J. Biomechanics*, Vol. 7, 1974, pp. 171-182.

14 Lee, J. M., and Boughner, D. R., "Tissue Mechanics of Canine Pericardium in Different Test Environments," *Circ. Res.*, Vol. 49, No. 2, 1981, pp. 533-544.

15 Lee, M. C., LeWinter, M. M., Freeman, G. L., Shabetai, R., and Fung, Y. C., "Biaxial Mechanical Properties of the Pericardium in Normal and Volume Overload Dogs," *Am. J. Physiol.*, Vol. 249, No. 2, 1985, pp. H222-230.

16 Rabkin, S. W., and Hsu, P. H., "Mathematical and Mechanical Modeling of Stress-strain Relationship of Pericardium," *Am. J. Physiol.*, Vol. 299, No. 4, 1975, pp. 896-900.

17 Tong, P., and Fung, Y. C., "The Stress-strain Relationship for the Skin," *J. Biomechanics*, Vol. 9, 1976, pp. 649-657.

18 Trowbridge, E. A., and Crofts, C. E., "The Standardization of Gauge Length: Its Influence on the Relative Extensibility of Natural and Chemically Modified Pericardium," *J. Biomechanics*, Vol. 12, 1986, pp. 1023-1033.

19 Vaishnav, R. N., Young, J. T., Janicki, J. S., and Patel, D. J., "Nonlinear Anisotropic Elastic Properties of the Canine Aorta," *Biophys. J.*, Vol. 12, 1972, pp. 1008-1027.

20 Vawter, D. L., Fung, Y. C., and West, J. B., "Constitutive Equation of Lung Tissue Elasticity," ASME JOURNAL OF BIOMECHANICAL ENGINEERING., Vol. 101, 1979, pp. 38-45.

21 Vito, R. P., "The Mechanical Properties of Soft Tissues—I: A Mechanical System for Biaxial Testing," *J. Biomechanics*, Vol. 13, No. 11, 1980, pp. 947-950.

22 Wiegner, A. W., and Bing, O. H. L., "Mechanical and Structural Correlates of Canine Pericardium," *Circ. Res.*, Vol. 49, No. 3, 1981, pp. 809-814.

23 Yin, F. C. P., Chew, P. H., and Zeger, S. L., "An Approach to Quantification of Biaxial Tissue Stress-strain Data," *J. Biomechanics.*, Vol. 19, No. 1, 1986, pp. 27-37.

24 Yin, F. C. P., Strumpf, R. K., Chew, P. H., and Zeger, S. L., "Quantification of the Mechanical Properties of Noncontracting Canine Myocardium under Simultaneous Biaxial Loading," *J. Biomechanics*, Vol. 20, No. 6, 1987, pp. 577-589.